

Bioglass incorporation improves mechanical properties and enhances cell-mediated mineralization on electrochemically aligned collagen threads

Madhura P. Nijsure,¹ Meet Pastakia,² Joseph Spano,^{2,3} Michael B. Fenn,^{2,3} Vipuil Kishore^{1,2,3}

¹Department of Chemical Engineering, Florida Institute of Technology, Melbourne, Florida 32901

²Department of Biomedical Engineering, Florida Institute of Technology, Melbourne, Florida 32901

³Center for Medical Materials and Biophotonics, Florida Institute of Technology, Melbourne, Florida 32901

Received 21 December 2016; revised 3 April 2017; accepted 26 April 2017

Published online 00 Month 2017 in Wiley Online Library (wileyonlinelibrary.com). DOI: 10.1002/jbm.a.36102

Abstract: Bone tissue engineering mandates the development of a functional scaffold that mimics the physicochemical properties of native bone. Bioglass 45S5 (BG) is a highly bioactive material known to augment bone formation and restoration. Hybrid scaffolds fabricated using collagen type I and BG resemble the organic and inorganic composition of the bone extracellular matrix and hence have been extensively investigated for bone tissue engineering applications. However, collagen–BG scaffolds developed thus far do not recapitulate the aligned structure of collagen found in native bone. In this study, an electrochemical fabrication method was employed to synthesize BG-incorporated electrochemically aligned collagen (BG-ELAC) threads that are compositionally similar to native bone. Further, aligned collagen fibrils within BG-ELAC threads mimic the anisotropic arrangement of collagen fibrils in native bone. The effect of BG incorporation on the mechanical properties and cell-mediated mineralization on ELAC threads was

investigated. The results indicated that BG can be successfully incorporated within ELAC threads, without disturbing collagen fibril alignment. Further, BG incorporation significantly increased the ultimate tensile stress (UTS) and modulus of ELAC threads ($p < 0.05$). SBF conditioning showed extensive mineralization on BG-ELAC threads that increased over time demonstrating the bone bioactivity of BG-ELAC threads. Additionally, BG incorporation into ELAC threads resulted in increased cell proliferation ($p < 0.05$) and deposition of a highly dense and continuous mineralized matrix. In conclusion, incorporation of BG into ELAC threads is a viable strategy for the development of an osteoconductive material for bone tissue engineering applications. © 2017 Wiley Periodicals, Inc. *J Biomed Mater Res Part A*: 00A:000–000, 2017.

Key Words: aligned collagen, bioglass, mineralization, bone tissue engineering

How to cite this article: Nijsure MP, Pastakia M, Spano J, Fenn MB, Kishore V. 2017. Bioglass incorporation improves mechanical properties and enhances cell-mediated mineralization on electrochemically aligned collagen threads. *J Biomed Mater Res Part A* 2017:00A:000–000.

INTRODUCTION

Physicochemical cues from the extracellular matrix (ECM) microenvironment have been shown to play a critical role in cell proliferation, migration, and tissue-specific differentiation.^{1–4} While several studies have attempted to develop biomimetic scaffolds that resemble individual facets of native bone ECM (i.e., composition, structure, or mechanics), little work is done on the fabrication of scaffolds that mimic multiple aspects of the bone ECM. For example, collagen–hydroxyapatite hybrid scaffolds resemble the composition of native bone^{5,6}; however, most existing scaffolds are mechanically weak with randomly oriented collagen fibers. On the other hand, electrospun aligned composites of poly(D,L-lactide-co-glycolide) (PLGA) and hydroxyapatite (HA) mimic the highly oriented ECM structure of native bone tissue, but are not compositionally similar.⁷ Development of a biomimetic scaffold

that recapitulates composition, mechanics, and anisotropic architecture of native bone is imperative to guide cell differentiation, and highly ordered cell-mediated *de novo* mineralization that is akin to the native tissue.⁸

Bioglass 45S5 (BG) is an osteostimulative glass ceramic that has been previously shown to be more bioactive compared to HA.^{9,10} Specifically, Oonishi et al. have shown that BG implantation into a critical sized bone defect in a rabbit model resulted in significantly faster bone restoration (2 weeks) compared to HA (12 weeks).¹⁰ Furthermore, controlled release of ions (e.g., Ca, Si) from BG have been shown to stimulate bone marrow stem cell differentiation,¹¹ osteoblast proliferation and differentiation,^{12–14} and matrix mineralization^{15,16}. Collagen type I and BG have been combined in numerous studies for the fabrication of biomimetic scaffolds for bone tissue engineering applications.¹⁷ While

Correspondence to: V. Kishore; e-mail: vkishore@fit.edu

Contract grant sponsor: College of Engineering, Florida Institute of Technology

pure collagen gel-based scaffolds are mechanically weak for use in load-bearing applications, incorporation of an inorganic phase within the collagen framework has been shown to structurally reinforce the collagen fibers and thereby significantly improve the mechanical properties of collagen-based scaffolds.^{18–20} Another limitation of collagen gels is the loosely packed network of collagen fibers resulting in low collagen fibrillar density compared to native bone. Unconfined plastic compression of collagen gels has been reported to densify collagen fibers and generate mechanically competent scaffolds that mimic the microstructural properties of the bone ECM.²¹ Furthermore, incorporation of BG within plastically compressed collagen matrices has been shown to expedite cell-mediated mineralization.^{15,22} Although plastic compression yields mechanically stiff and dense collagen scaffolds, the collagen fibers in these scaffolds are randomly oriented and do not mimic the aligned collagen network found in native bone. Therefore, there is a need for an alternative collagen densification method that yields highly oriented collagen-BG scaffolds for bone tissue engineering applications.

In this study, an electrochemical method based on the principles of isoelectric focusing was employed to synthesize BG incorporated electrochemically aligned collagen (BG-ELAC) threads. To the best of our knowledge, this is the first attempt to incorporate BG particles into aligned collagen network. Native bone is a composite mixture of 50–70% inorganic mineral and 20–40% organic matrix that is mostly comprised of collagen type I.^{23,24} BG-ELAC threads developed in this study mimic the compositional and structural (highly aligned and densely packed collagen fibers) aspects of the native bone ECM niche. In this study, two different hypotheses were tested: (1) tissue-level (60 wt %) BG can be incorporated within aligned collagen threads using the electrochemical process, and (2) BG incorporation will enhance mechanical properties and cell-mediated mineralization on electrochemically aligned collagen (ELAC) threads. BG incorporation into ELAC threads was confirmed via Alizarin red S staining and Raman spectroscopy. The effect of BG incorporation on the alignment of ELAC threads was assessed by polarized microscopy. Monotonic tensile tests were performed to assess the effect of BG incorporation on the mechanical properties of ELAC threads. Bone bioactivity of BG-ELAC threads was demonstrated by assessing the formation of hydroxycarbonate apatite (HCA) layer post incubation in simulated body fluid (SBF) using scanning electron microscopy (SEM).²⁵ Finally, Saos-2 cells were cultured on BG-ELAC threads and osteoblastic activity was assessed via examination of cell-mediated mineralization using SEM, energy dispersive X-ray spectroscopy (EDAX) and Raman spectroscopy.

MATERIALS AND METHODS

Synthesis of bioglass-incorporated ELAC threads

BG was incorporated within ELAC threads by following a previously published protocol with slight modifications.^{26,27} Briefly, acid soluble monomeric type I bovine collagen solution (Purecol, 3.1 mg/mL, Advanced Biomatrix, CA) was dialyzed against water for 24 h. A stock solution of BG particles (46.1 mol % SiO₂, 26.9 mol % CaO, 24.4 mol % Na₂O, 2.5 mol % P₂O₅; GLO160P/-20; ~20 μm particle size; MO-SCI

Corporation, MO) was prepared by suspending the particles at a concentration of 200 mg/mL in water. An appropriate volume of BG particles was suspended into dialyzed collagen solution to make a composite mixture of BG:collagen 60:40 (w/w). The BG:collagen mixture was loaded between two stainless-steel wire electrodes (electrode spacing: 1.8 mm) and an electric field of 3 V was applied for 30 min. The electric field triggers the formation of a pH gradient between the electrodes resulting in the collagen molecules close to the anode gaining a positive charge and the ones close to the cathode gaining a negative charge. The like-charged electrodes repel the collagen molecules away resulting in aggregation of the collagen molecules at the isoelectric point (pI). During the alignment process, the BG particles become entrapped within aligned collagen to form BG-ELAC threads. Collagen-only threads were prepared in a similar manner but without the addition of BG particles. ELAC and BG-ELAC threads were freshly prepared for all the experiments. In case of overnight storage, excess water was blotted on a Kim Wipe and the threads were stored in a semi-wet condition in the refrigerator at 4°C. The term thread is used in this study to signify bundles of densely packed collagen microfibrils within ELAC.

Confirmation of bioglass incorporation within ELAC threads via Alizarin Red S staining

Alizarin Red S is commonly used to identify the presence of calcium in tissue sections.²⁸ As BG is rich in calcium, the presence of BG within ELAC threads can be confirmed by staining the BG-ELAC threads with Alizarin Red S. ELAC threads (without BG) were used as control. Threads were stained with 40 mM Alizarin Red S stain for 20 min at room temperature and washed with copious amounts of water to remove excess dye. Following this, the threads were imaged under a microscope to examine the presence and distribution of BG in BG-ELAC threads.

Effect of bioglass incorporation on alignment of ELAC threads

Polarized imaging was employed to assess the effect of BG incorporation on the alignment of ELAC threads as described in a previous publication.²⁹ Briefly, BG-ELAC threads were placed on a polarized microscope (Zeiss) equipped with a first-order wavelength gypsum plate. The alignment of collagen molecules within BG-ELAC threads was confirmed by verifying that the birefringent collagen molecules appear blue when the thread was aligned parallel to the slow axis of the gypsum plate.

Quantitative assessment of amount of bioglass incorporated within ELAC threads

While 60 wt % BG was initially added to dialyzed collagen solution prior to the electrochemical alignment process, it is important to confirm the amount of BG that is incorporated within ELAC thread postalignment. As ELAC and BG-ELAC threads were made using the same volume of collagen solution, it was assumed that the amount of collagen present in the threads was the same. At first, ELAC threads (16 cm length; *N* = 4/group) were vacuum dried, weighed

individually (W_{ELAC}), and the average dry weight of ELAC thread ($W_{ELAC, avg}$) was calculated. BG-ELAC threads of the same length ($N = 4$) were weighed ($W_{BG-ELAC}$) in a similar manner. The amount of BG incorporated (W_{BG}) was calculated by taking the difference in weight of each BG-ELAC thread with the average weight of ELAC threads ($W_{BG-ELAC} - W_{ELAC, avg}$). The amount of BG per gram of BG-ELAC thread was calculated by taking the ratio of the weight of BG and the total weight of BG-ELAC using the equation below.

$$W_{BG} \text{ per gram of thread} = \frac{W_{BG-ELAC} - W_{ELAC, avg}}{W_{BG-ELAC}}$$

To determine the stability of BG particles within the thread, ELAC and BG-ELAC threads were incubated in calcium free PBS for 7 days at 37 °C. At periodic intervals (day 1, day 3, and day 7), threads were removed from the incubator, vacuum dried, and weighed. The weights recorded were used to determine whether BG particles remain intact in an aqueous medium over time.

Mechanical assessment of bioglass-incorporated ELAC threads

The effect of BG incorporation on the mechanical properties of ELAC threads was assessed by performing monotonic tensile tests using a Q800 dynamic mechanical analyzer (TA Instruments). At first, each thread was cut at 2 cm length. Excess water was removed by lightly blotting each thread on a kim wipe. To minimize physical handling of the threads, they were glued at both ends onto transparency sheets. The threads were rehydrated and the cross-sectional areas of ELAC and BG-ELAC threads ($N = 27/\text{group}$) was determined by imaging the threads on a Zeiss microscope and then measuring the diameter of each thread using image analysis (Image J). Monotonic tensile tests were performed by mounting the thread onto tension clamps. An initial preload force of 0.001 N was applied to ensure that the threads are taut prior to loading. Following this, the thread was loaded at a rate of 0.01 N/min until failure and the load and displacement data were recorded.³⁰ The loading rate employed in this study was optimized based on a few pilot samples to ensure that the samples remain fully hydrated during the test and the true wet mechanical properties can be determined. Stress was computed by normalizing the load with the initial cross-sectional area of the thread and strain was determined by taking the ratio of the change in length to the original length. Stress-strain curves were generated and ultimate tensile stress (UTS) and ultimate strain (US) were determined. Tensile modulus was calculated by taking the slope of the steepest region of the stress-strain curve.

Assessment of mineralization of bioglass-incorporated ELAC threads in SBF

The bone bioactivity of ELAC and BG-ELAC threads was assessed by incubating the threads in Kokubo's simulated body fluid (SBF). SBF was prepared by following the recipe

published by Kokubo et al. and the pH of SBF was adjusted to 7.4.²⁵ SBF conditioning of the threads (1 cm length) was performed by incubating the threads in sterile SBF in microcentrifuge tubes at 37°C for 7 days. The recommended ratio of SBF volume to surface area of the threads was maintained throughout the incubation period²⁵ and the SBF solution was replaced every two days to replenish the supply of ions. At periodic intervals (days 1, 3, and 7), threads were removed from SBF ($N = 3/\text{group}/\text{time point}$), washed with DI water and prepared for SEM analysis. Briefly, the threads were dehydrated in a graded series of ethanol (20%, 50%, 75%, 90%, and 100%) and then treated with 50:50 v/v amyl acetate:ethanol solution, and stored in 100% amyl acetate. The threads were then dried in a Denton DCP-1 critical point dryer, sputter-coated with gold, and observed under SEM (JEOL SEM).

Saos-2 cell culture

Human Osteosarcoma Saos-2 cells (HTB-85, ATCC) were cultured in 75 cm² flasks and maintained in RPMI growth medium (Corning, VA) supplemented with 15% fetal bovine serum (FBS), 1% L-glutamine, and 1% penicillin-streptomycin in 5% CO₂ at 37°C. Passage-7 cells were used for all the experiments.

Effect of bioglass incorporation into ELAC threads on Saos-2 cell viability, morphology, and proliferation

ELAC and BG-ELAC threads were cut into 2-cm-long pieces, sterilized in 70% ethanol, washed in 1× PBS, and placed in an ultralow attachment 6-well plate (6 threads/well). To assess the effect of BG incorporation on cell viability and morphology, saos-2 cells (passage 7) were seeded onto the threads at a density of 10,000 cells/cm² (based on the area of the well). The unattached cells were removed 6 h post-seeding by replacing the culture medium and the adherent cells were cultured for 7 days. The cells were maintained in osteogenic medium composed of alpha-MEM supplemented with 10% FBS, 1% L-glutamine, 1% penicillin/streptomycin, 50 µg/mL ascorbic acid, and 10 mM β-glycerophosphate. Culture medium was replaced every 3 days.

For cell viability assessment, threads were extracted from the culture plate ($N = 3$ threads/group/time point) at day 1 and day 7, washed in PBS and stained with Calcein AM (live cells) and ethidium homodimer (dead cells) for 15 min at 37°C. Following this, the stained cells were imaged using a fluorescent microscope (Zeiss) to assess cell viability.

For cell morphology assessment, threads were extracted ($N = 3$ threads/group/time point) from the culture wells at days 1 and 7, and fixed with 3.7% formaldehyde solution (with 0.05% Triton-X 100 in 1× PBS) for 15 min at room temperature. The threads were then washed with PBS and incubated in permeabilization buffer (0.1% Triton-X 100 in 1× PBS) for 15 min. After permeabilization, the threads were washed twice with 1× PBS and incubated in blocking buffer (1% bovine serum albumin and 0.05% Triton-X 100 in 1× PBS) for 30 min. Following this, the threads were washed with PBS, and the cells were stained with a working solution (1:25 dilution in 1× PBS) of AlexaFluor

488 Phalloidin (Invitrogen, CA) for 30 min. Confocal microscopy (Nikon) was performed to image the cell cytoskeleton and assess cell morphology on ELAC and BG-ELAC threads.

Cell proliferation was quantified using Alamar Blue assay. At days 1, 4, and 7, threads were incubated in a 10% Alamar blue solution in culture medium at 37°C for 2 h. Aliquots of 100 μ L from each well were transferred to a 96-well plate in triplicate and fluorescence was measured at an excitation wavelength of 555 nm and emission wavelength of 595 nm using M2e Spectramax plate reader (Molecular Devices). A standard curve was generated using known cell populations and the resulting equation was used to calculate the cell numbers on the threads.

Assessment of cell-mediated mineralization using SEM and EDAX analyses

To assess the effect of BG incorporation into ELAC threads on Saos-2 cell-mediated mineralization, SEM analyses was performed. At day 7, threads were extracted from culture wells ($N = 3$ threads/group) and fixed in 2.5% glutaraldehyde solution (in $1\times$ PBS) for 3 h. Following this, the threads were dehydrated and dried as described in the section "Assessment of mineralization of bioglass-incorporated ELAC threads in SBF." SEM analysis was performed to visually confirm the presence of mineralized nodules on ELAC and BG-ELAC threads. Furthermore, EDAX analyses were performed to assess the composition of cell-mediated mineralized matrix.

Raman characterization of bioglass-incorporated ELAC threads

Raman spectroscopy was used to confirm the presence of BG within the ELAC threads as prepared. Additionally, the degree of Saos-2 cell-mediated apatite formation was also investigated after 7 days of culture. At day 7, ELAC threads were removed from culture wells, fixed in 3.7% formalin, washed with $1\times$ PBS, and subsequently prepared for Raman analysis by placing the threads onto MgF_2 slides (Crystran, UK) submerged in PBS. The Raman system utilized in this study for imaging and spectral acquisition included a Renishaw InVia Raman Spectrometer (Renishaw PLC, UK) coupled to an upright Leica DM2500 microscope with an automated XYZ stage and fluorescence imaging system. The spectrometer consists of a 785 nm NIR Diode laser, 1200 l/mm grating, and a 1" Deep Depletion CCD camera. A $63\times$ Leica U-V-I water dipping objective lens with 0.9 NA and 2 mm working distance was used for all spectral acquisitions. The StreamlineHR mapping function within the Renishaw Wire 4.2 software was utilized to collect line maps ($N = 12$) for each group of ELAC threads from a wavenumber range of approximately 600–1700 cm^{-1} . Each line map consisted of 10 acquisitions using an 8 μ m step size for a total sampling length of 80 μ m per line map. An acquisition time of 15 s was used for all maps collected. All the spectra then underwent preprocessing, which includes a fitted polynomial baseline subtraction for background removal, and cosmic ray removal using the "width of features" identification procedure within the Wire 4.2 software. A total of 2 line maps were rejected from the

dataset as outliers associated with instrumentation anomalies. Average spectra, standard deviations, and difference spectra were then calculated and plotted using Matlab (Mathworks).

Statistical analyses

Normality of data was assessed using JMP software (JMP Statistical Discovery from SAS, Cary, NC). Data for mechanical tests of ELAC and BG-ELAC threads were found to be non-normal. Therefore, a nonparametric statistical analysis was performed using the Wilcoxon test (JMP). Data for Alamar blue assay was normally distributed and hence statistical analyses to assess differences in cell number between ELAC and BG-ELAC threads at each time point was performed using one-way ANOVA with Tukey *post hoc* test (JMP). Statistical significance was set at $p < 0.05$.

RESULTS

Characterization of bioglass-incorporated ELAC threads

ELAC threads without BG showed no evidence of Alizarin red S staining [Fig. 1(A)]. On the other hand, BG-ELAC threads stained positive for Alizarin red S confirming that BG can be successfully incorporated throughout the length of the ELAC threads by simply mixing it with dialyzed collagen prior to the electrochemical process [Fig. 1(B)]. Raman spectral data showed that subtraction of the average collagen-only ELAC thread spectrum from the average BG-ELAC thread spectrum yields the spectral contribution from the initial incorporation of the BG [Fig. 1(C)]. The peak at 960 cm^{-1} originates from the strong phosphate stretching mode of the BG composition,^{15,31,32} suggesting BG has been successfully incorporated into the ELAC threads. Furthermore, the 960 cm^{-1} peak is not observed for spectra collected from the collagen-only ELAC thread, as would be expected, as no BG was incorporated.

Polarized imaging showed that the collagen molecules in BG-ELAC threads exhibit blue color when aligned parallel to the slow axis of the gypsum plate suggesting that collagen alignment in ELAC is maintained upon BG incorporation (Fig. 2).

Quantification of bioglass amount in ELAC threads

The average dry weight of a 16-cm-long ELAC thread ($W_{ELAC, avg}$) was found to be 0.6 ± 0.1 mg. On the other hand, the dry weight of individual BG-ELAC threads ($W_{BG-ELAC}$) of the same length ranged from 1.2 to 1.6 mg. The average amount of BG (W_{BG}) incorporated in a 16-cm-long BG-ELAC thread was found to be 0.87 ± 0.15 mg ($W_{BG-ELAC} - W_{ELAC, avg}$). Finally, the amount of BG incorporated per gram of BG-ELAC thread was calculated by taking the ratio of W_{BG} to $W_{BG-ELAC}$ and found to be 0.59 ± 0.06 g ($\sim 60\%$ w/w) suggesting that most of the BG added to dialyzed collagen is incorporated within the ELAC thread after the electrochemical process. Together, these results indicate that the electrochemical process is a highly efficient method for the incorporation of BG within aligned collagen threads.

Furthermore, no change in the weights of ELAC and BG-ELAC threads was found over time (data not shown) suggesting that the ions release slowly from BG and that BG particles were stably present within the threads until day 7.

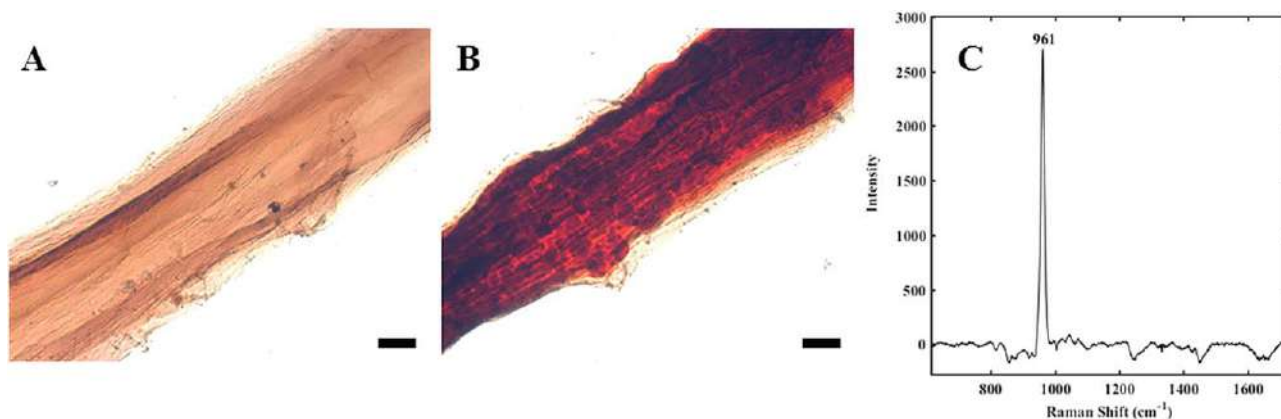


FIGURE 1. A,B: Confirmation of BG incorporation in ELAC threads with Alizarin Red S staining. BG-ELAC thread stained positive for Alizarin Red S (B) while ELAC threads without BG did not stain red (A). Scale bar: 100 μm . C: Raman difference spectra indicating the contribution of initial BG incorporation, resulting from the subtraction of average collagen-only ELAC thread spectra from average BG-ELAC thread spectra as made. The strong peak at 961 cm^{-1} corresponds to characteristic PO_4^{3-} vibrations within BG.

Effect of bioglass incorporation on mechanical properties of ELAC threads

Monotonic tensile tests were performed to evaluate the mechanical properties of ELAC and BG-ELAC threads. Figure 3(A) shows the typical stress-strain curves obtained for ELAC and BG-ELAC threads. BG incorporation resulted in a significant increase in the UTS and tensile modulus of ELAC threads ($p < 0.05$). Specifically, a threefold increase in UTS [Fig. 3(B)] and a fivefold increase in the tensile modulus [Fig. 3(C)] were observed upon incorporation of BG into ELAC threads. On the other hand, the extensibility of BG-ELAC threads was significantly lower ($p < 0.05$) compared to ELAC threads as indicated by an ultimate strain (US) of 15% for BG-ELAC threads compared to 30% for ELAC threads [Fig. 3(D)]. Together, these results indicate that BG incorporation significantly improves the strength and modulus of ELAC threads.

Effect of bioglass incorporation into ELAC threads on mineralization in SBF

Mineralization in SBF was investigated using SEM to assess the bone bioactivity of ELAC and BG-ELAC threads. SEM imaging revealed that mineralization of BG-ELAC threads was

initiated at day 1 and threads on day 1 that was observed to progressively increase with time [Fig. 4(D-F)]. By day 7, extensive mineralization was observed throughout the length of the BG-ELAC threads [Fig. 4(F)]. On the other hand, ELAC threads showed no evidence of mineralization until day 7 [Fig. 4(A-C)]. Together, these results indicate that incorporation of BG improves the bone bioactivity of ELAC threads.

Effect of bioglass incorporation into ELAC threads on saos-2 cell viability, morphology, and proliferation

Results from live-dead assay showed that almost all cells stained green at day 1 and day 7 on both ELAC and BG-ELAC threads (Fig. 5), indicating that Saos-2 cells are viable on both groups. Confocal images of actin cell cytoskeletal staining revealed that the cells were uniformly seeded on both ELAC and BG-ELAC threads at day 1 [Fig. 6(A,D)]. No discernible differences in cell morphology were observed between the two thread types. Furthermore, cells on both the threads showed preferential orientation along the long axis of the thread suggesting that the underlying topography of the threads is guiding cell alignment. Comparing the cell actin filament staining between day 1, day 4, and day 7

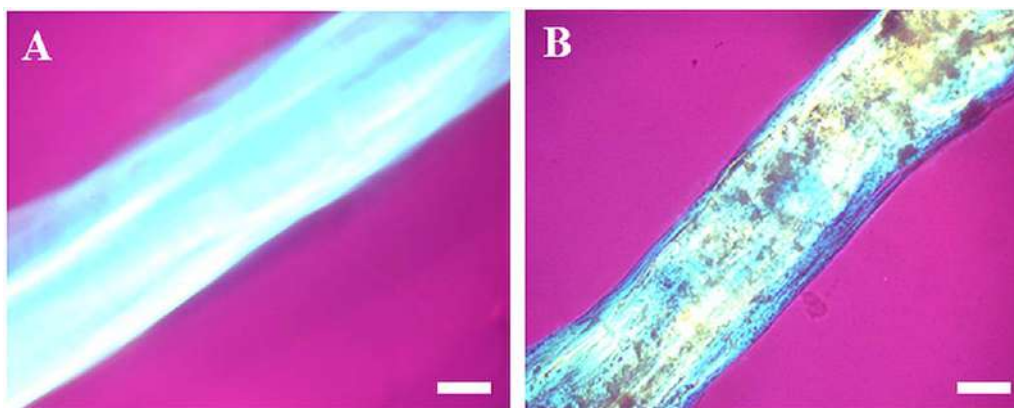


FIGURE 2. Polarized imaging of ELAC (A) and BG-ELAC (B) threads. BG incorporation does not disturb the alignment of collagen fibrils in ELAC threads. Scale bar: 100 μm .

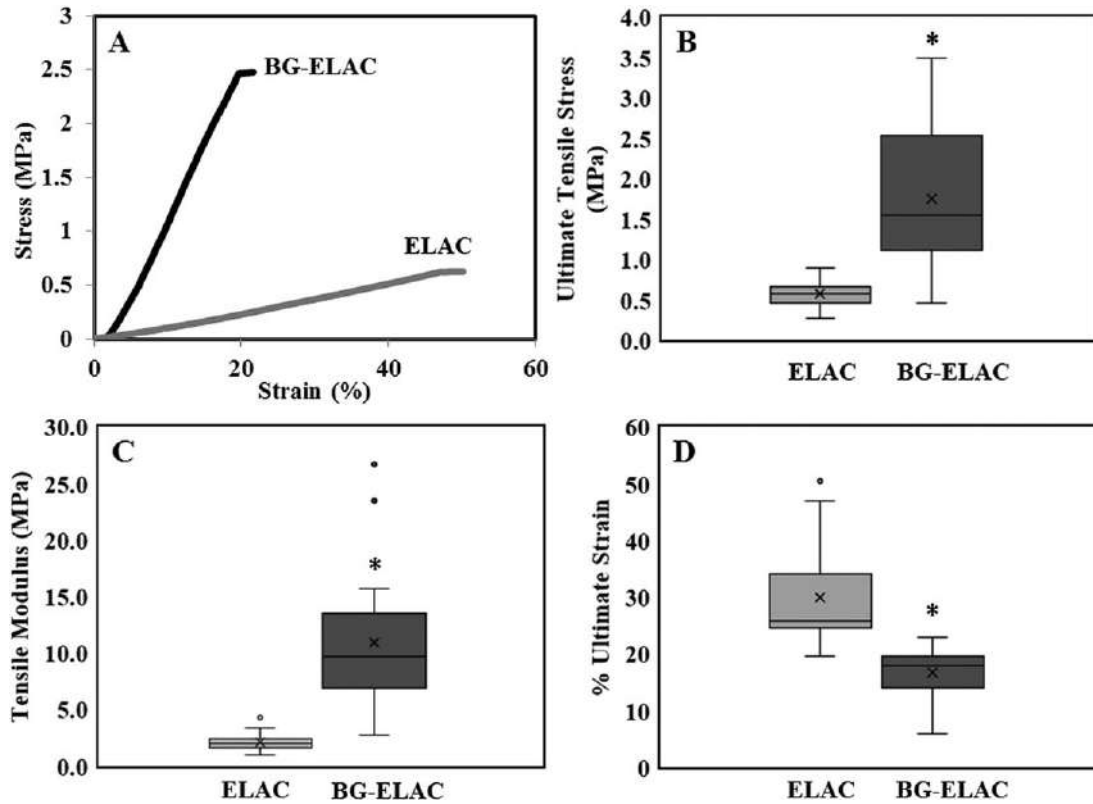


FIGURE 3. Assessment of mechanical properties of ELAC and BG-ELAC threads. A: Typical stress–strain curves for ELAC and BG-ELAC threads. B: Ultimate tensile stress. C: Tensile modulus. D: Ultimate strain. The boxes represent 25th to 75th percentile of the data separated by a line at the median. The whiskers show the upper and lower extremes. Dots show the outliers. BG incorporation significantly increases the ultimate tensile stress and the tensile modulus of ELAC threads. * indicates statistical significance $p < 0.05$ between ELAC and BG-ELAC threads.

clearly shows that cells proliferate rapidly over time on both ELAC and BG-ELAC threads (Fig. 6). By day 7, a fully confluent cell layer was observed on both threads indicating that cells proliferate well on both threads [Fig. 6(C,F)]. Alamar blue results showed that the cell numbers on BG-ELAC

threads were significantly ($p < 0.05$) higher than ELAC threads suggesting that BG incorporation increased Saos-2 cell proliferation (Fig. 7). Together, these results indicate that viability, morphology, and proliferation of Saos-2 cells are maintained on BG-ELAC threads.

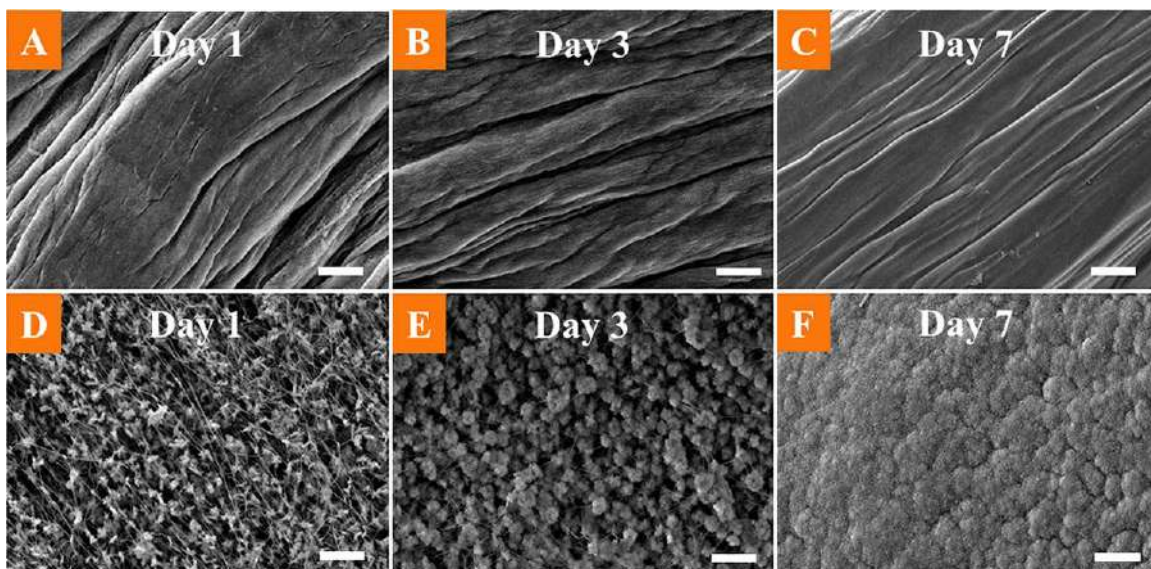


FIGURE 4. SEM analysis of mineralization on ELAC and BG-ELAC threads after conditioning in SBF. A,B,C: ELAC threads do not show mineralization after 7 days of conditioning in SBF. D,E,F: SEM imaging showed increased mineralization in BG-ELAC threads over time. Scale bar: 5 μm .

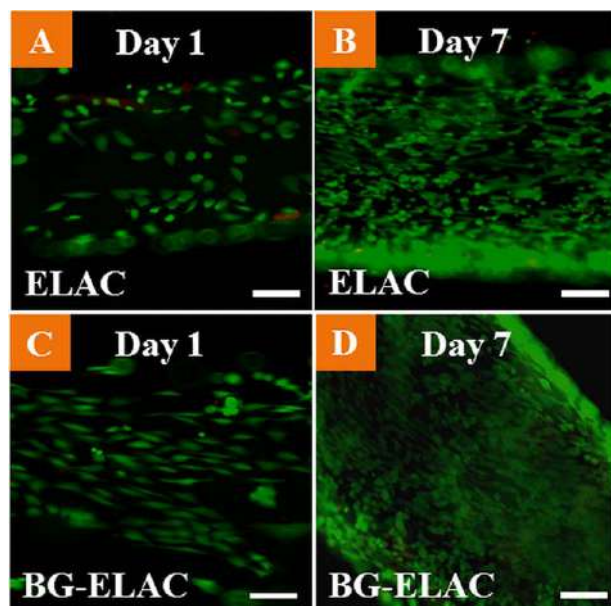


FIGURE 5. Assessment of Saos-2 cell viability using live-dead assay. Most of the cells appear green indicating that cells are viable until day 7 on ELAC and BG-ELAC threads. Scale bar: 100 μm .

Effect of bioglass incorporation into ELAC threads on saos-2 cell-mediated mineralization

Cell-mediated mineralization on ELAC and BG-ELAC threads was assessed using SEM and EDAX analyses. While little to no mineralization was observed on ELAC threads [Fig. 8(A,D)], a highly dense layer of mineralized matrix was observed on BG-ELAC threads [Fig. 8(B,E)]. SEM images

revealed the presence of numerous matrix-vesicle-like structures on Saos-2 cells seeded on BG-ELAC threads [Fig. 8(E)]. On the other hand, cells seeded on ELAC threads showed very few of these structures [Fig. 8(D)]. EDAX analyses of the mineralized matrix on BG-ELAC threads showed distinct peaks for Ca and P with a Ca/P ratio of 1.4 [Fig. 9(B)]. Ca and P peaks were not observed on ELAC threads [Fig. 9(A)]. BG-ELAC threads without cells also showed some evidence of mineralization [Fig. 8(C,F)]; however, the extent of mineralization was significantly lower than that on BG-ELAC threads with cells [Fig. 8(B,E)]. Furthermore, EDAX analyses revealed that the mineralized matrix on BG-ELAC threads with cells was compositionally richer in Ca and P [34 wt % Ca and 18 wt % P; Fig. 9(B)] compared to the matrix on BG-ELAC threads without cells (11 wt % Ca and 7 wt % P; Fig. 9(C)). Together, these results indicate that BG incorporation enhances Saos-2 cell-mediated mineralization on ELAC threads thereby confirming the bone bioactivity of BG-ELAC threads.

Confirmation of cell-mediated mineralization by Raman spectroscopy

The 960 cm^{-1} peak intensity observed for BG-ELAC threads before culture provides for an initial reference value for subsequent comparison to the BG/apatite spectral contribution after cell culture. Shown in Figure 10(A) is the difference spectrum produced by subtraction of the average spectrum collected from cell-free BG-ELAC threads incubated in cell culture media for 7 days from the average spectrum of the cell seeded BG-ELAC threads after 7 days in culture. Therefore, Figure 10(A) provides the spectral

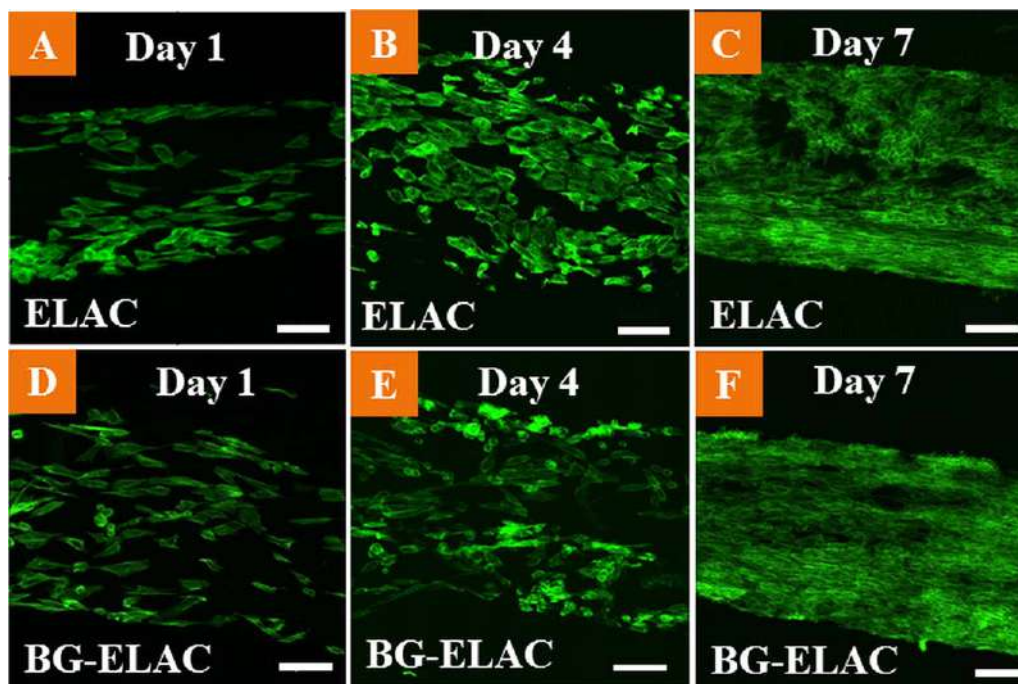


FIGURE 6. Assessment of Saos-2 cell morphology on ELAC and BG-ELAC threads via cytoskeleton staining using Alexa Fluor Phalloidin 488. No differences in cell morphology were observed between two thread types. Cells proliferate well on both threads and a fully confluent cell layer is observed on day 7. Scale bar: 100 μm .

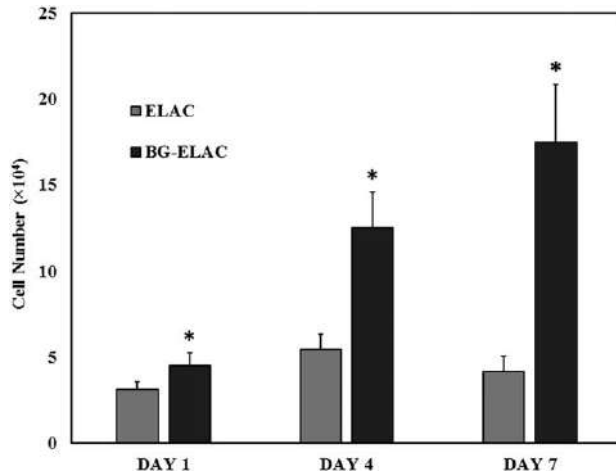


FIGURE 7. Quantification of cell proliferation on ELAC and BG-ELAC threads using Alamar blue assay. BG incorporation enhanced cell proliferation on ELAC threads. * indicates $p < 0.05$ between ELAC and BG-ELAC threads at each time point.

change due to the presence of cells on the BG-ELAC threads after 7 days of culture, giving the overall cellular contribution. Evidence of the spectral contribution from the cells is suggested by the presence of the 1005 cm^{-1} peak often used as an indicator of cellular protein content.³² Notably, it appears that there is an overall significant increase in the intensity of the 960 cm^{-1} peak, which may suggest that apatite nodule formation by the cells is contributing to the increased phosphate peak intensity. This suggestion is further evidenced by inspection of Figure 10(B) which shows

the overlay of the average spectrum from BG-ELAC threads at before cell culture and the average spectrum from BG-ELAC threads at day 7 after cell culture. From the spectral overlay, it can be seen that not only is the 960 cm^{-1} peak area significantly greater after 7 days of cell culture, but also the 960 cm^{-1} peak exhibits a broadening with a shoulder becoming present at 936 cm^{-1} . This may suggest further that the increased peak area is due to the presence of not only the original BG, but also the spectral contribution from a surface layer of apatite in the form of nodules as revealed by SEM imaging and EDAX analyses.

DISCUSSION

BG is a highly bioactive material that has been reported to bond to both bone and soft tissue.³³ Low fracture toughness of pure BG scaffolds is a major limitation that impedes their use in load-bearing applications.³⁴ Development of composite scaffolds comprising a polymeric biomaterial and BG can help improve toughness and yet maintain the bioactivity associated with BG. Collagen type I and BG composite scaffolds mimic the compositional aspects of native bone and hence have been extensively investigated for bone tissue engineering applications.¹⁷ Freeze-drying^{35,36} and plastic compression^{15,22} are commonly used scaffold fabrication methodologies for the synthesis of collagen-BG scaffolds. Freeze-drying yields highly porous BG-incorporated collagen scaffolds but these scaffolds are mechanically weak. While cross-linking improves the mechanical properties of freeze-dried scaffolds,³⁷ it can significantly modulate the host response to the scaffold upon implantation.³⁸ On the other

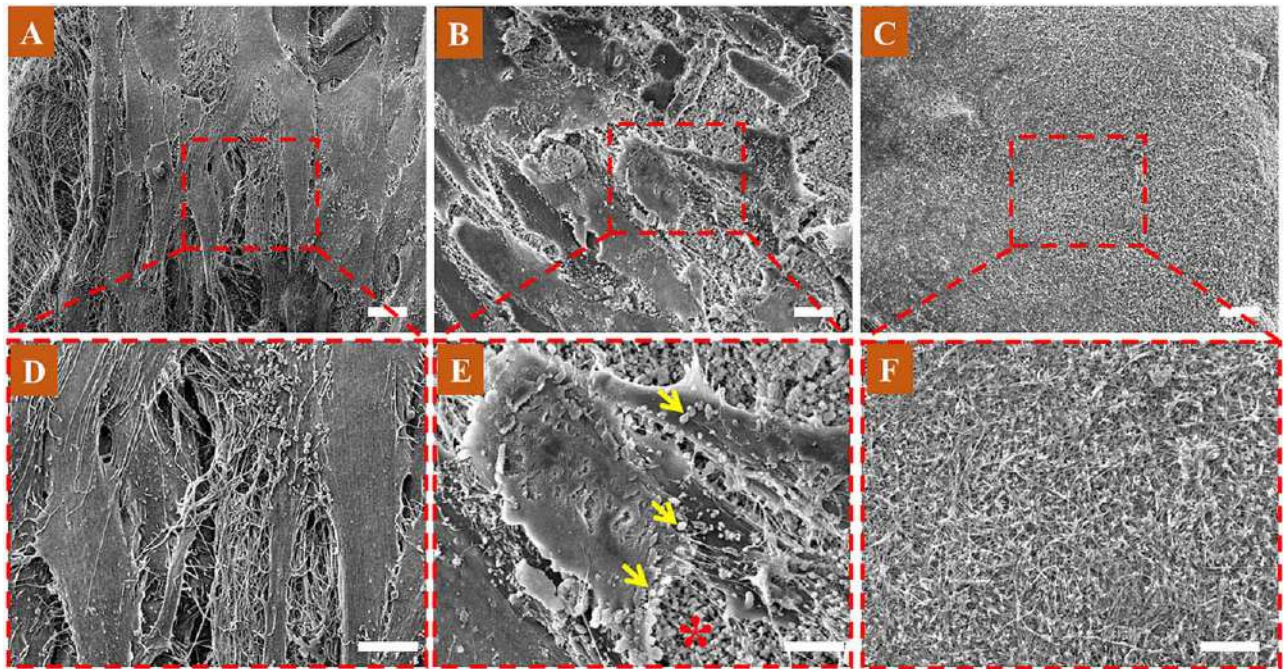


FIGURE 8. Assessment of Saos-2 cell-mediated mineralization on ELAC and BG-ELAC threads after 7 days. A–C: Low-magnification images (scale bar: $10\text{ }\mu\text{m}$). D–F: High-magnification images (scale bar: $5\text{ }\mu\text{m}$). A,D: Saos-2 cells seeded on ELAC threads showed no evidence of mineralization in culture. B,E: Cells seeded on BG-ELAC threads showed the formation of characteristic mineralized nodules on the cell surface, along with the deposition of a dense cell-mediated mineralized matrix (indicated by “**”). The arrow heads point to vesicle-like structures on the cell surface. (C, F) Extent of mineralization on BG-ELAC threads in culture medium without cells was significantly lower than with cells (B, E).

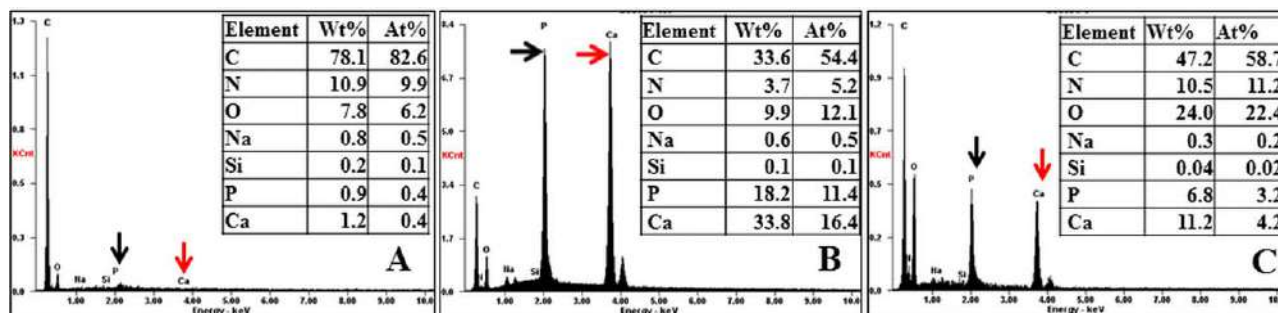


FIGURE 9. EDAX analysis of Saos-2 cell-mediated mineralization on ELAC and BG-ELAC threads. A: ELAC thread did not show the presence of calcium or phosphorus peaks. The cell-mediated matrix deposited on the BG-ELAC thread (B) was compositionally richer in calcium and phosphorous as compared to (C) the mineralization observed on BG-ELAC threads incubated in culture medium without cells at day 7 (Ca peaks: red arrows; P peaks: black arrows).

hand, plastic compression of BG incorporated collagen gels provides a highly dense and mechanically stiff collagen matrix³⁹; however, unlike native bone, the collagen fibers within the plastically compressed matrix are randomly oriented. Previous studies have shown that anisotropically oriented collagen fibers can act as a framework for cell-mediated deposition of an oriented mineralized matrix that is similar to the structural arrangement of mineralized fibers found in native bone.^{8,40} Several methods that include extrusion,^{41,42} electrospinning,^{43,44} microfluidic alignment,⁴⁵ and magnetic alignment^{46,47} have been employed to develop collagen-based scaffolds with anisotropically aligned collagen fibers. However, to the best of our knowledge, use of these methodologies to incorporate an insoluble second phase within the aligned collagen network is not straightforward. We have previously shown that it is feasible to incorporate additional components (e.g., decorin, elastin) within highly aligned and dense

collagen matrices using the electrochemical fabrication technology by simply mixing the component with collagen prior to the electrochemical process.^{26,27,48} This study is the first attempt to incorporate BG into ELAC threads in an effort to mimic the compositional, structural, and functional properties of native bone and thereby allow for better integration of the scaffold with host tissue to augment bone repair and regeneration.

Electrochemical fabrication methodology is a pH-gradient-driven process for the synthesis of highly aligned collagen threads via the application of an electric field that drives the self-assembly of the collagen molecules along the isoelectric point.²⁹ This method has been previously used to synthesize collagen scaffolds for tendon,^{49,50} cornea,⁵¹ vascular,²⁷ and nerve⁵² tissue engineering applications. In this study, 60% of BG (w/w) was incorporated within ELAC thread to mimic the 60% inorganic (mineral) and 40% organic (collagen)

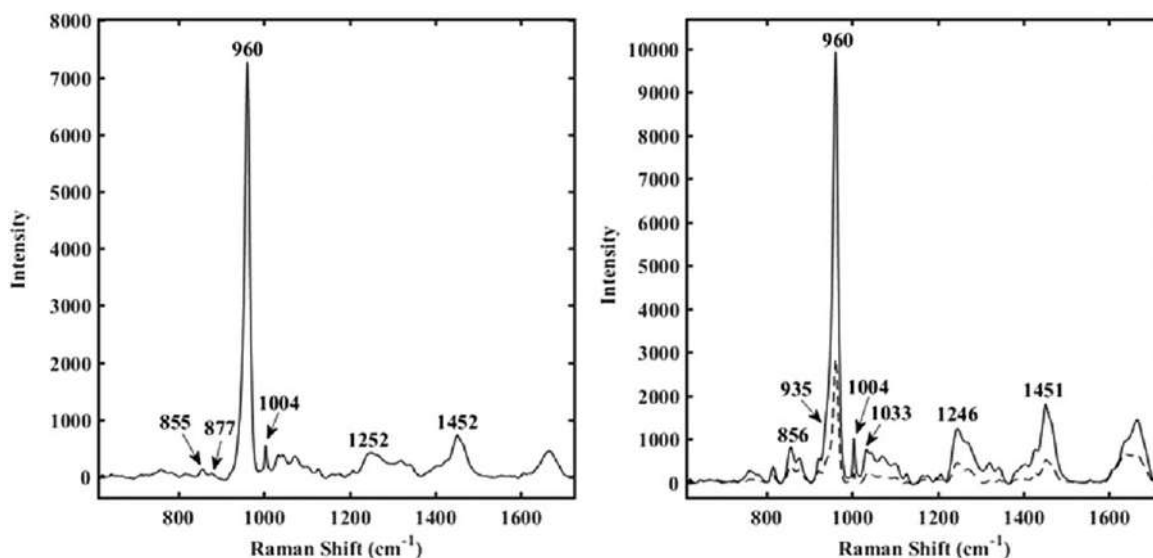


FIGURE 10. Raman spectra confirming cell-mediated mineralization on BG incorporated ELAC threads after 7 days of incubation. A: Difference spectra indicating the overall cellular contribution after 7 days of incubation, produced by subtracting the average spectra of cell-free day 7 BG-ELAC threads from cell seeded day 7 BG-ELAC threads. The presence of a peak at 1004 cm^{-1} and a high-intensity phosphate peak at 960 cm^{-1} suggest the presence of cellular protein and apatite formation. B: Overlay spectra of as made BG-ELAC thread average spectra (shown with dashed line) and cell-seeded BG-ELAC threads after 7 days of culture (shown with solid line). A significant increase in 960 cm^{-1} peak intensity is observed, and the formation of a broad shoulder in the 935 cm^{-1} region. Collagen peaks can be observed at 856, 877, 1033, 1246, and 1451 cm^{-1} . The sharp peak at 1004 cm^{-1} can be assigned to phenylalanine ring vibrations.

composition of native bone.^{23,24} BG incorporation within ELAC threads was confirmed via Alizarin red S staining [Fig. 1(B)] as has been previously done with plastically compressed collagen matrices.¹⁶ Polarized microscopy revealed that collagen alignment within the ELAC thread is maintained upon BG incorporation (Fig. 2). This finding is in contrast to a previous study that showed that incorporation of decorin at moderately high concentrations (10:1 collagen:decorin molar ratio) resulted in significant disruption of collagen alignment within ELAC threads.²⁶ This disruption in collagen alignment upon decorin incorporation was attributed to the lateral aggregation and precipitation of collagen fibrils mediated by the interaction of dermatan sulfate and collagen in low ionic conditions like the ones present in dialyzed collagen.⁵³ These aggregates are large in size and hence fail to orient along the long axis of the ELAC thread. On the other hand, the BG particles get physically entrapped within the core of the ELAC threads without inducing aggregation of collagen fibrils and thus the overall alignment of collagen in BG-ELAC threads is maintained.

The amount of BG incorporated within ELAC threads was quantified by calculating the percent difference in the weights of BG-ELAC and ELAC threads of equal length. A similar method has been previously employed to quantify the amount of collagen and BG in plastically compressed collagen matrices.²² Results from this study showed that most of the BG particles added to dialyzed collagen get entrapped within the ELAC thread suggesting that the electrochemical process is a highly efficient method for the generation of collagen-based composite materials. It must be noted that the BG amount calculated in this study is a reasonable estimate based on the assumption that the mass of collagen in ELAC and BG-ELAC threads is comparable.

Highly ordered and densely packed arrangement of collagen fibers are critical for the load-bearing mechanical properties of musculoskeletal tissues such as bone and tendon. Collagen fibrils within ELAC threads mimic this arrangement and hence show improved mechanical properties as compared to traditional gel-based collagen scaffolds which are weak due to poor packing density and random orientation of collagen fibers.²⁹ Tensile test results from this study showed that BG incorporation significantly increased the mechanical properties of ELAC threads (Fig. 3). These results are in agreement with several studies in the literature that show an increase in tensile strength and modulus of collagen-based scaffolds upon BG incorporation.^{18,54} Wheeler et al. have shown that composites of elastin-like polypeptides (ELP) and collagen showed a two- to threefold increase in the tensile modulus after BG incorporation.⁵⁴ In another study, Long et al. incorporated BG into a macroporous collagen fiber scaffold using a slurry dipping technique and showed that the tensile strength and modulus of the scaffold significantly increased upon BG incorporation.¹⁸ This enhancement in mechanical properties can be attributed to the formation of a composite collagen-BG structure that results in the reinforcement of the collagen fiber framework.^{17,20} Further, it has been previously reported that interfacial interactions between collagen and BG improves

the tensile properties of collagen-BG scaffolds.¹⁸ Although the tensile modulus of BG-ELAC threads is weaker than native bone (1–20 GPa),⁵⁵ the mechanical properties of BG-ELAC threads are significantly higher than most other collagen-BG scaffolds possibly due to the anisotropic orientation of collagen fibrils within BG-ELAC threads. Specifically, the tensile modulus of BG-ELAC threads investigated in this study was around 10 MPa, which is significantly higher than that reported for plastically compressed collagen-BG matrices (1.2 MPa).¹⁶ Furthermore, the aligned collagen topography within BG-ELAC threads can promote cell adhesion and oriented matrix deposition via contact guidance.

Results from the SBF study showed extensive mineralization on BG-ELAC threads while no mineralization ensued on ELAC threads (Fig. 4). This selective mineralization only on the BG-ELAC threads can be attributed to the well-established mechanism for the formation of hydroxyl-carbonate-apatite (HCA) layer via ionic dissolution from BG followed by chemisorption of amorphous Ca^{2+} , PO_4^{3-} , and CO_3^{2-} ions to form hydroxyapatite crystallites that act as nucleation sites for crystallization of the HCA layer.⁵⁶ Previous studies have shown that the HCA layer readily bonds with type I collagen and thereby strengthens the interaction between collagen and BG particles.^{57,58} Specifically, Orefice et al. have performed AFM measurements and shown that the magnitude of interaction between collagen and BG particles is directly dependent on the amount of HCA layer formation.^{57,58} SBF results of the current study are in agreement with previous work that assessed the bone bioactivity of plastically compressed collagen-BG scaffolds and showed that the presence of BG induced rapid mineralization in SBF.²² In a separate study, a porous composite scaffold using polylactide-co-glycolide (PLAGA) and BG was shown to induce the formation calcium phosphate deposits in SBF suggesting that the incorporation of BG improved the bioactivity of the PLAGA scaffold.²⁰ Expedited mineralization in SBF demonstrates the bioactivity of BG-ELAC threads and may serve as a predictive indicator of the in vivo performance of BG-ELAC threads for bone tissue engineering applications.

Saos-2 cells are mature osteoblasts that readily mineralize in vitro and hence have been used as a model by several studies to assess the osteoconductivity of materials.^{59–62} The enhanced cell proliferation on ELAC threads upon BG incorporation (Fig. 7) is in agreement with a previous study that showed that dissolution of ionic products from BG improves cell proliferation.⁶³ SEM results from this study showed evidence of some mineralization on BG-ELAC threads incubated for 7 days in culture medium without cells possibly due to the precipitation of Ca and P ions from the cell culture media [Fig. 8(C,F)]. When Saos-2 cells were cultured on BG-ELAC threads, extensive mineralization was observed as evidenced by a dense and continuous layer of mineralized nodules surrounding the cells under SEM [Fig. 8(B,E)]. On the other hand, little to no cell-mediated mineralization was observed on ELAC threads without BG [Fig. 8(A,D)]. Matrix-vesicle-like structures were predominantly observed on the surface of Saos-2 cells seeded on BG-ELAC

threads [Fig. 8(E)]. Previous studies have demonstrated that the formation of matrix vesicles is indicative of the onset of cell-mediated mineralization.^{64,65} Matrix vesicles are not as prominent on ELAC threads without BG [Fig. 8(D)], suggesting that the mineralization process on ELAC threads is a lot slower than that observed on BG-ELAC threads. A possible mechanism for enhanced Saos-2 cell-mediated mineralization on BG-ELAC threads may be associated with the accumulation of ions released from BG within the cell vesicles followed by subsequent budding and release of these vesicles onto the collagen thread network and formation of calcium phosphate deposits.⁶⁶ These deposits in turn act as nucleation sites that crystallize into a mineralized matrix in the presence of Ca and P ions from BG and in the surrounding culture medium.⁶⁷ EDAX analyses showed higher calcium and phosphorous composition on BG-ELAC threads with cells compared to without cells suggesting the formation of a more mature cell-mediated mineralized matrix [Fig. 9(B,C)]. The Raman spectral overlay data show a significantly greater 960 cm^{-1} peak for BG-ELAC threads after 7 days in culture [Fig. 10(B)], a finding that corroborates with EDAX analyses and confirms enhanced mineralization in the presence of cells.

In conclusion, electrochemical fabrication methodology can be employed to incorporate tissue-level BG into aligned collagen threads and yield a biomimetic material that resembles the compositional and structural properties of native bone. Results from the SBF study together with Saos-2 cell-mediated mineralization demonstrated that BG incorporation improves the osteoconductivity of ELAC threads. We have previously shown that pure ELAC threads suppress osteogenic differentiation of mesenchymal stem cells (MSCs).⁴⁹ Future studies will investigate whether incorporation of BG stimulates osteogenic differentiation of MSCs on ELAC threads. Such material-directed osteogenic differentiation may eliminate the need for external factors (e.g., BMP-2, dexamethasone) as a viable growth factor-free approach for bone repair and regeneration. Further, application of the electrochemical method is not limited to aligned threads alone but can also be used to synthesize compacted collagen sheets by employing planar electrodes.⁴⁸ The collagen fibers within these sheets are densified but not anisotropically aligned. Assessment of MSC osteogenic differentiation on BG-incorporated electrochemically fabricated aligned and unaligned collagen matrices will allow for decoupling the effects of collagen alignment and BG incorporation on cellular response. Overall, BG-ELAC threads have immense potential to be used as an osteoconductive material for bone tissue engineering applications.

ACKNOWLEDGMENTS

The authors would like to acknowledge Ms Gayle Duncombe at the High Resolution Microscopy and Imaging Center for her help with SEM and confocal microscopy. We would also like to thank MO-SCI Corporation for their kind donation of the BG used in this study.

REFERENCES

- Burdick JA, Vunjak-Novakovic G. Engineered microenvironments for controlled stem cell differentiation. *Tissue Eng A* 2008;15:205–219.
- Engler AJ, Sen S, Sweeney HL, Discher DE. Matrix elasticity directs stem cell lineage specification. *Cell* 2006;126:677–689.
- Ghasemi-Mobarakeh L, Prabhakaran MP, Tian L, Shamirzaei-Jeshvaghani E, Dehghani L, Ramakrishna S. Structural properties of scaffolds: Crucial parameters towards stem cells differentiation. *World J Stem Cells* 2015;7:728–744.
- Gurkan UA, Cheng X, Kishore V, Uquillas JA, Akkus O. Comparison of morphology, orientation, and migration of tendon derived fibroblasts and bone marrow stromal cells on electrochemically aligned collagen constructs. *J Biomed Mater Res A* 2010;94:1070–1079.
- Villa MM, Wang L, Huang J, Rowe DW, Wei M. Bone tissue engineering with a collagen-hydroxyapatite scaffold and culture expanded bone marrow stromal cells. *J Biomed Mater Res B Appl Biomater* 2015;103:243–253.
- Al-Munajjed AA, Plunkett NA, Gleeson JP, Weber T, Jungreuthmayer C, Levingstone T, Hammer J, O'Brien FJ. Development of a biomimetic collagen-hydroxyapatite scaffold for bone tissue engineering using a SBF immersion technique. *J Biomed Mater Res B Appl Biomater* 2009;90:584–591.
- Jose MV, Thomas V, Johnson KT, Dean DR, Nyairo E. Aligned PLGA/HA nanofibrous nanocomposite scaffolds for bone tissue engineering. *Acta Biomater* 2009;5:305–315.
- Lanfer B, Seib FP, Freudenberg U, Stamov D, Bley T, Bornhäuser M, Werner C. The growth and differentiation of mesenchymal stem and progenitor cells cultured on aligned collagen matrices. *Biomaterials* 2009;30:5950–5958.
- Oonishi H, Kushitani S, Yasukawa E, Iwaki H, Hench LL, Wilson J, Tsuji E, Sugihara T. Particulate bioglass compared with hydroxyapatite as a bone graft substitute. *Clin Orthop Relat Res* 1997;(334):316–325.
- Oonishi H, Hench LL, Wilson J, Sugihara F, Tsuji E, Matsuura M, Kin S, Yamamoto T, Mizokawa S. Quantitative comparison of bone growth behavior in granules of bioglass, A-W glass-ceramic, and hydroxyapatite. *J Biomed Mater Res* 2000;51:37–46.
- Bosetti M, Cannas M. The effect of bioactive glasses on bone marrow stromal cells differentiation. *Biomaterials* 2005;26:3873–3879.
- Xynos I, Hukkanen M, Batten J, Buttery L, Hench L, Polak J. Bioglass[®] 45S5 stimulates osteoblast turnover and enhances bone formation in vitro: Implications and applications for bone tissue engineering. *Calcif Tissue Int* 2000;67:321–329.
- Xynos ID, Edgar AJ, Buttery LD, Hench LL, Polak JM. Ionic products of bioactive glass dissolution increase proliferation of human osteoblasts and induce insulin-like growth factor II mRNA expression and protein synthesis. *Biochem Biophys Res Commun* 2000;276:461–465.
- Xynos ID, Edgar AJ, Buttery LD, Hench LL, Polak JM. Gene-expression profiling of human osteoblasts following treatment with the ionic products of Bioglass[®] 45S5 dissolution. *J Biomed Mater Res* 2001;55:151–157.
- Marelli B, Ghezzi CE, Mohn D, Stark WJ, Barralet JE, Boccaccini AR, Nazhat SN. Accelerated mineralization of dense collagen-nano bioactive glass hybrid gels increases scaffold stiffness and regulates osteoblastic function. *Biomaterials* 2011;32:8915–8926.
- Liu G, Pastakia M, Fenn MB, Kishore V. Saos-2 cell-mediated mineralization on collagen gels: Effect of densification and bioglass incorporation. *J Biomed Mater Res A* 2016;104:1121–1134.
- Sarker B, Hum J, Nazhat SN, Boccaccini AR. Combining collagen and bioactive glasses for bone tissue engineering: A review. *Adv Healthcare Mater* 2015;4:176–194.
- Long T, Yang J, Shi S, Guo Y, Ke Q, Zhu Z. Fabrication of three-dimensional porous scaffold based on collagen fiber and bioglass for bone tissue engineering. *J Biomed Mater Res B Appl Biomater* 2015;103:1455–1464.
- Lee JH, El-Fiqi A, Han C, Kim H. Physically-strengthened collagen bioactive nanocomposite gels for bone: A feasibility study. *Tissue Eng Regen Med* 2015;12:90–97.
- Lu HH, El-Amin SF, Scott KD, Laurencin CT. Three-dimensional, bioactive, biodegradable, polymer-bioactive glass composite scaffolds with improved mechanical properties support collagen synthesis and mineralization of human osteoblast-like cells in vitro. *J Biomed Mater Res A* 2003;64:465–474.

21. Brown RA, Wiseman M, Chuo CB, Cheema U, Nazhat SN. Ultra-rapid engineering of biomimetic materials and tissues: Fabrication of nano- and microstructures by plastic compression. *Adv Funct Mater* 2005;15:1762–1770.
22. Marelli B, Ghezzi CE, Barralet JE, Boccaccini AR, Nazhat SN. Three-dimensional mineralization of dense nanofibrillar collagen-bioglass hybrid scaffolds. *Biomacromolecules* 2010;11:1470–1479.
23. Clarke B. Normal bone anatomy and physiology. *Clin J Am Soc Nephrol* 2008;3 Suppl 3:S131–S139.
24. Boskey AL. Erratum: Bone composition: Relationship to bone fragility and antiosteoporotic drug effects. *Bonekey Rep* 2015;4:710.
25. Kokubo T, Takadama H. How useful is SBF in predicting in vivo bone bioactivity? *Biomaterials* 2006;27:2907–2915.
26. Kishore V, Paderi JE, Akkus A, Smith KM, Balachandran D, Beaudoin S, Panitch A, Akkus O. Incorporation of a decorin biomimetic enhances the mechanical properties of electrochemically aligned collagen threads. *Acta Biomater* 2011;7:2428–2436.
27. Nguyen TU, Bashour CA, Kishore V. Impact of elastin incorporation into electrochemically aligned collagen fibers on mechanical properties and smooth muscle cell phenotype. *Biomed Mater* 2016;11:025008–6041/11/025008.
28. Puchtler H, Meloan SN, Terry MS. On the history and mechanism of alizarin and alizarin red S stains for calcium. *J Histochem Cytochem* 1969;17:110–124.
29. Cheng X, Gurkan UA, Dehen CJ, Tate MP, Hillhouse HW, Simpson GJ, Akkus O. An electrochemical fabrication process for the assembly of anisotropically oriented collagen bundles. *Biomaterials* 2008;29:3278–3288.
30. Bitar M, Salih V, Brown RA, Nazhat SN. Effect of multiple unconfined compression on cellular dense collagen scaffolds for bone tissue engineering. *J Mater Sci Mater Med* 2007;18:237–244.
31. Notingher I, Boccaccini A, Jones J, Maquet V, Hench L. Application of Raman microspectroscopy to the characterisation of bioactive materials. *Mater Charact* 2002;49:255–260.
32. Hench LL, Roki N, Fenn MB. Bioactive glasses: Importance of structure and properties in bone regeneration. *J Mol Struct* 2014;1073:24–30.
33. Jones JR. Review of bioactive glass: From Hench to hybrids. *Acta Biomater* 2013;9:4457–4486.
34. Fu Q, Saiz E, Rahaman MN, Tomsia AP. Bioactive glass scaffolds for bone tissue engineering: State of the art and future perspectives. *Mater Sci Eng C* 2011;31:1245–1256.
35. Xu C, Su P, Chen X, Meng Y, Yu W, Xiang AP, Wang Y. Biocompatibility and osteogenesis of biomimetic bioglass-collagen-phosphatidylserine composite scaffolds for bone tissue engineering. *Biomaterials* 2011;32:1051–1058.
36. Yang C, Wang Y, Chen X. Mineralization regulation and biological influence of bioactive glass-collagen-phosphatidylserine composite scaffolds. *Sci China Life Sci* 2012;55:236–240.
37. Wang Y, Yang C, Chen X, Zhao N. Development and characterization of novel biomimetic composite scaffolds based on bioglass-collagen-hyaluronic acid-phosphatidylserine for tissue engineering applications. *Macromol Mater Eng* 2006;291:254–262.
38. Badylak SF. The extracellular matrix as a scaffold for tissue reconstruction. *Cell Develop Biol* 2002;13:377.
39. Neel EAA, Cheema U, Knowles JC, Brown RA, Nazhat SN. Use of multiple unconfined compression for control of collagen gel scaffold density and mechanical properties. *Soft Matter* 2006;2:986–992.
40. Caliri SR, Harley BA. Structural and biochemical modification of a collagen scaffold to selectively enhance MSC tenogenic, chondrogenic, and osteogenic differentiation. *Adv Healthcare Mater* 2014;3:1086–1096.
41. Zeugolis DI, Paul GR, Attenburrow G. Cross-linking of extruded collagen fibers—A biomimetic three-dimensional scaffold for tissue engineering applications. *J Biomed Mater Res A* 2009;89:895–908.
42. Pins GD, Christiansen DL, Patel R, Silver FH. Self-assembly of collagen fibers. Influence of fibrillar alignment and decorin on mechanical properties. *Biophys J* 1997;73:2164–2172.
43. Zhong S, Teo WE, Zhu X, Beuerman RW, Ramakrishna S, Yung LYL. An aligned nanofibrous collagen scaffold by electrospinning and its effects on in vitro fibroblast culture. *J Biomed Mater Res A* 2006;79:456–463.
44. Zeugolis DI, Khew ST, Yew ES, Ekaputra AK, Tong YW, Yung LL, Huttmacher DW, Sheppard C, Raghunath M. Electro-spinning of pure collagen nano-fibres—just an expensive way to make gelatin? *Biomaterials* 2008;29:2293–2305.
45. Lee P, Lin R, Moon J, Lee LP. Microfluidic alignment of collagen fibers for in vitro cell culture. *Biomed Microdevices* 2006;8:35–41.
46. Guo C, Kaufman LJ. Flow and magnetic field induced collagen alignment. *Biomaterials* 2007;28:1105–1114.
47. Torbet J, Malbouyres M, Builles N, Justin V, Roulet M, Damour O, Oldberg Å, Ruggiero F, Hulmes DJ. Orthogonal scaffold of magnetically aligned collagen lamellae for corneal stroma reconstruction. *Biomaterials* 2007;28:4268–4276.
48. Younesi M, Islam A, Kishore V, Panit S, Akkus O. Fabrication of compositionally and topographically complex robust tissue forms by 3D-electrochemical compaction of collagen. *Biofabrication* 2015; (in press).
49. Kishore V, Bullock W, Sun X, Van Dyke WS, Akkus O. Tenogenic differentiation of human MSCs induced by the topography of electrochemically aligned collagen threads. *Biomaterials* 2012;33:2137–2144.
50. Denning D, Abu-Rub M, Zeugolis D, Habelitz S, Pandit A, Fertala A, Rodriguez BJ. Electromechanical properties of dried tendon and isoelectrically focused collagen hydrogels. *Acta Biomater* 2012;8:3073–3079.
51. Kishore V, Iyer R, Frandsen A, Nguyen T. In vitro characterization of electrochemically compacted collagen matrices for corneal applications. *Biomed Mater* 2016;11:055008.
52. Abu-Rub MT, Billiar KL, van Es MH, Knight A, Rodriguez BJ, Zeugolis DI. Nano-textured self-assembled aligned collagen hydrogels promote directional neurite guidance and overcome inhibition by myelin associated glycoprotein. *Soft Matter* 2011;7:2770–2781.
53. Öbrink B. The influence of glycosaminoglycans on the formation of fibers from monomeric tropocollagen in vitro. *Eur J Biochem* 1973;34:129–137.
54. Wheeler TS, Sbravati ND, Janorkar AV. Mechanical & cell culture properties of elastin-like polypeptide, collagen, bioglass, and carbon nanosphere composites. *Ann Biomed Eng* 2013;41:2042–2055.
55. Rho J, Kuhn-Spearing L, Zioupos P. Mechanical properties and the hierarchical structure of bone. *Med Eng Phys* 1998;20:92–102.
56. Will J, Gerhardt L, Boccaccini AR. Bioactive glass-based scaffolds for bone tissue engineering. In: Anonymous Tissue Engineering III: Cell-Surface Interactions for Tissue Culture. Springer; 2011. p 195–226.
57. Hench LL, Greenspan D. Interactions between bioactive glass and collagen: A review and new perspectives. *J Aust Ceram Soc* 2013; 49:1–40.
58. Orefice R, Hench L, Brennan A. Evaluation of the interactions between collagen and the surface of a bioactive glass during in vitro test. *J Biomed Mater Res A* 2009;90:114–120.
59. Schröder HC, Boreiko O, Krasko A, Reiber A, Schwertner H, Müller WE. Mineralization of SaOS-2 cells on enzymatically (silicatein) modified bioactive osteoblast-stimulating surfaces. *J Biomed Mater Res B Appl Biomater* 2005;75:387–392.
60. Saino E, Grandi S, Quartarone E, Maliardi V, Galli D, Bloise N, Fassina L, De Angelis M, Mustarelli P, Imbriani M. In vitro calcified matrix deposition by human osteoblasts onto a zinc-containing bioactive glass. *Eur Cell Mater* 2011;21:59–72.
61. Wang X, Tolba E, Schroder HC, Neufurth M, Feng Q, Diehl-Seifert B, Muller WE. Effect of bioglass on growth and biomineralization of SaOS-2 cells in hydrogel after 3D cell bioprinting. *PLoS One* 2014;9:e112497.
62. Czekanska E, Stoddart M, Richards R, Hayes J. In search of an osteoblast cell model for in vitro research. *Eur Cell Mater* 2012;24:1–17.
63. Valerio P, Pereira MM, Goes AM, Leite MF. The effect of ionic products from bioactive glass dissolution on osteoblast proliferation and collagen production. *Biomaterials* 2004;25:2941–2948.
64. Golub EE. Role of matrix vesicles in biomineralization. *Biochim Biophys Acta* 2009;1790:1592–1598.
65. Wuthier RE, Lipscomb GF. Matrix vesicles: Structure, composition, formation and function in calcification. *Front Biosci* 2011;16: 2812–2902.
66. Wang X, Schröder HC, Schlossmacher U, Neufurth M, Feng Q, Diehl-Seifert B, Müller WE. Modulation of the initial mineralization process of SaOS-2 cells by carbonic anhydrase activators and polyphosphate. *Calcif Tissue Int* 2014;94:495–509.
67. Anderson HC. Matrix vesicles and calcification. *Curr Rheumatol Rep* 2003;5:222–226.